EXPERIMENTAL CVD SYNTHETIC DIAMONDS FROM LIMHP-CNRS, FRANCE

Wuyi Wang, Alexandre Tallaire, Matthew S. Hall, Thomas M. Moses,
Jocelyn Achard, Ricardo S. Sussmann, and Alix Gicquel

In the last decade, progress in diamond growth by chemical vapor deposition (CVD) has resulted in significant improvement in the quality of synthetic single crystals. This article reports on the gemological and spectroscopic features of six synthetic type IIa diamonds grown for research purposes at the French Laboratoire d'Ingénierie des Matériaux et des Hautes Pressions (LIMHP-CNRS), and compares their diagnostic features to CVD-grown diamonds from other producers. Three of the six samples were nitrogen doped, whereas the other three were classified as high purity. A number of characteristics that are diagnostic of CVD synthetic diamond were present in the nitrogen-doped crystals, despite an absence of defect-related absorption features in the infrared region. Identification of the high-purity samples was more complicated, but it was still possible based on features in their photoluminescence spectra, their distinctive birefringence, and characteristic luminescence images.

Diamond synthesis was first accomplished more than half a century ago, and there have been considerable improvements in quality over the past few years. These achievements are important not only for the potential they offer for producing large quantities of synthetic diamond, but also for the precise control they provide over the type and concentration of defects in the crystals, which is particularly critical for electronics applications. To date, most gem-quality synthetic diamonds have been grown using high-pressure and high-temperature (HPHT) conditions (Shigley et al., 1986, 1987, 1997, 2003, 2004). Recently, however, single-crystal diamond synthesis using the chemical vapor deposition (CVD) method has made great progress and attracted much attention, even in the jewelry industry (see, e.g., Yan et al., 2002; Wang et al., 2003; Martineau et al., 2004; Bates, 2005; Tallaire et al., 2005). Earlier this year, Yan et al. (2005) documented the successful growth of a 5 ct single-crystal CVD synthetic diamond measuring over 1 cm thick. They also predicted that a one-inch cube of single-crystal CVD synthetic diamond (~300 ct) is achievable. The properties of CVD synthetic diamonds are highly variable, due to the rapid development of laboratory synthesis techniques. Therefore, the timely characterization of these synthetic diamonds is critical to the gem industry.

In this article, we report on the properties and identification features of several CVD synthetic diamonds that were produced for research purposes at the Laboratoire d'Ingénierie des Matériaux et des Hautes Pressions, a part of the Centre National de la Recherche Scientifique (LIMHP-CNRS) at the Université Paris 13. These products showed some notable differences from those grown by Apollo Diamond Co. that were examined by Wang et al. (2003) and the experimental products studied by Martineau et al. (2004). Nevertheless, these new CVD-grown diamonds can be identified on the basis of certain characteristic gemological and spectroscopic features.

At LIMHP-CNRS, these CVD synthetic diamonds were produced at low pressures (a few hundred millibars) from hydrogen-rich methane mix-

See end of article for About the Authors and Acknowledgments.
GEMS & GEMOLOGY, Vol. 41, No. 3, pp. 234–244.
© 2005 Gemological Institute of America

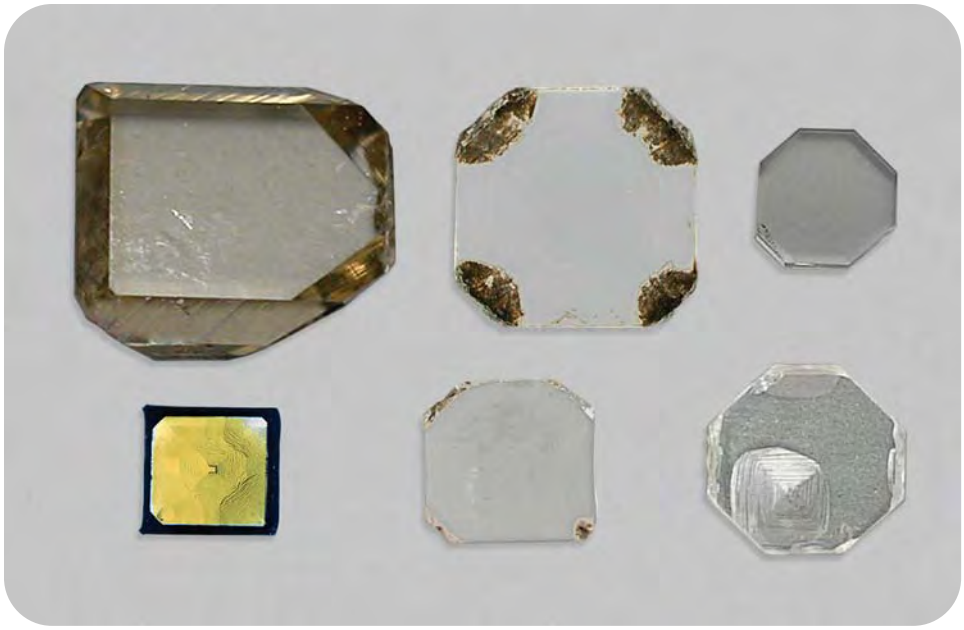


Figure 1. The CVD synthetic diamonds (0.14–0.81 ct) from LIMHP-CNRS show a typical tabular crystal morphology and significant variations in color. Three samples were near colorless, two were light gray, and one was light brown. The three samples in the top row (from left to right: nos. 67404, 66875, and 66669) are nitrogen doped, and the three in the bottom row (from left to right: nos. 66675, 66876, and 67405) are of high purity. Sample no. 66675 appears yellow due to the yellow substrate. Composite of photos by Elizabeth Schrader, Jessica Arditi, and W. Wang.

tures. The use of microwave radiation in the growth chamber facilitated the production of key molecular species involved in diamond growth inside the plasma ball. To grow a monocrystalline diamond crystal, a type Ib {100}-oriented slice of HPHT synthetic diamond was used as a substrate. By choosing optimum growth conditions for the substrate temperature, the methane concentration, and the microwave power density, researchers at LIMHP-CNRS were able to achieve growth rates of tens of micrometers per hour at relatively high quality and purity (Tallaire et al., 2005). These samples were grown solely for research purposes, and although it is technically possible to do so, no crystals thick enough to be faceted were produced. While colorless, light gray, and light brown gem-quality CVD-grown synthetic diamonds are being produced experimentally by LIMHP-CNRS, this group does not intend to make its synthetic diamonds available to the jewelry market.

MATERIALS AND METHODS

Six specimens produced by LIMHP-CNRS during late 2004 and early 2005, ranging from 0.14 to 0.81 ct, were examined (figure 1). All were studied as-grown, with no secondary treatment. Three of them were intentionally doped with various concentrations of nitrogen during the CVD deposition process in order to improve the growth rates. These samples were labeled nos. 67404, 66875, and 66669 for the very low, low, and moderate doping amounts, respectively. For the other three samples, the growth conditions were chosen to limit the incorporation of defects into the crystal lattice as much as possible. They are referred to here as nos. 66675, 66876, and 67405. The growth substrates were entirely removed prior to spectroscopic analysis as well as color grading during this study, except for one high-purity sample that had a CVD thickness of only about 0.3 mm (no. 66675). These CVD synthetic diamonds are representative of recent products created at LIMHP-CNRS, which show a significant variation in color and chemical purity.

Gemological and spectroscopic properties of all six samples were collected at the GIA Laboratory in New York. Although GIA does not issue grading reports on synthetic diamonds, for the purpose of this study equivalent color grades were determined by experienced diamond grading staff using the standard conditions and methodology of GIA's color grading system for colored and near-colorless faceted diamonds (see, e.g., King et al., 1994). Note that the color grades of these tabular samples could change after faceting as the optical path length is increased. Internal features were observed with a standard binocular microscope and a variety of lighting techniques. We used a gemological microscope with crossed polarizers to check for anomalous birefringence in all samples. Reactions to UV radiation were checked in a darkened room with a conventional four-watt combination long-wave (365 nm) and short-wave (254 nm) lamp.

Five of the samples also were analyzed at the GIA Laboratory using several spectroscopic techniques. Because the substrate of no. 66675 was not removed, only photoluminescence (PL) spectroscopy was per-

TABLE 1. Characteristics of CVD synthetic diamonds from LIMHP-CNRS, France.[a]

Sample no.	Description	N_2 doping during growth	Weight (ct)	Size (mm)	Color	UV fluorescence[b]	Fluorescence in the DiamondView
Nitrogen doped							
67404	Free standing	Very low	0.81	6.55 × 5.96 × 1.64	Light brown	Inert	Orange (with blue phosphorescence)
66875	Free standing	Low	0.41	6.33 × 6.27 × 0.70	Light gray	Inert	Orangy red (with blue at four corners)
66669	Free standing	Medium	0.31	3.99 × 3.87 × 1.42	"G" color	Inert	Orangy red
High purity							
66675	About 0.3 mm thick, over HPHT synthetic diamond substrate	None	0.40	3.88 x 3.86 x 1.87	Near colorless (over yellow substrate)	nd	Green (from the substrate)
66876	Free standing	None	0.14	4.41 × 4.42 × 0.48	Light gray	Inert	Blue
67405	Free standing	None	0.18	4.47 × 4.46 × 0.71	"I" color	Inert	Blue (with blue phosphorescence)

[a] *Abbreviation: nd = not determined*
[b] *Reaction to a standard gemological source of long- and short-wave UV radiation*

formed on this sample. To avoid surface contamination, we cleaned the samples thoroughly with acetone in an ultrasonic bath. Low-temperature PL spectra were recorded for all six samples using a Renishaw 1000 Raman microspectrometer with an Ar-ion laser at two different laser excitations: 488.0 nm (for the range 490–950 nm) and 514.5 nm (for the range 517–950 nm). PL spectra in the range 640–1000 nm also were collected using a He-Ne laser (632.8 nm) for the five samples that had their substrate removed. In addition, PL spectra for one sample (no. 67405) were obtained using a diode laser (780.0 nm) for the range 782–1000 nm. Several excitation lasers were used to cover as broad an emission-energy region as possible. The samples were cooled by direct immersion in liquid nitrogen. Up to three scans were accumulated in some cases to achieve a better signal-to-noise ratio.

Infrared absorption spectra were recorded in the mid-IR (6000–400 cm^{-1}, 1.0 cm^{-1} resolution) and near-IR (up to 11000 cm^{-1}, 4.0 cm^{-1} resolution) regions at room temperature with a Thermo-Nicolet Nexus 670 Fourier-transform infrared spectrometer equipped with KBr and quartz beam splitters. A 6× beam condenser focused the incident beam on the sample, and a total of 1,024 scans (per spectrum) were collected to improve the signal-to-noise ratio.

UV-Vis-NIR absorption spectra were recorded with a Thermo-Spectronic Unicam UV500 spectrophotometer over the range 250–850 nm with a sampling interval of 0.1 nm. The samples were mounted in a cryogenic cell and cooled using liquid nitrogen.

All the samples also were examined using a Diamond Trading Company (DTC) DiamondView deep-ultraviolet (<230 nm) luminescence imaging system (Welbourn et al., 1996).

RESULTS AND DISCUSSION

Gemological Features. Table 1 details the gemological and spectroscopic properties of the LIMHP-CNRS synthetic diamonds. All six crystals exhibited the tabular morphology typical of monocrystalline CVD products, each with a large cubic (100) crystal face. Three of the samples were near colorless, two were light gray, and one was light brown (again, see figure 1). The colors of these samples are very different from those of the Apollo CVD synthetic diamonds, most of which showed brown colors of varying saturation (Wang et al., 2003). The one brown sample in this study (no. 67404) showed an even color distribution, except when viewed perpendicular to the growth direction; in this orientation a distinct zone of dark brown color was visible (figure 2). This very narrow color zone extended parallel to the large (100) face

Major absorption features		Photoluminescence features
Infrared	UV-Vis-NIR	
6856, 3323, 3124, 2924, 2807 cm^{-1}	Increase in absorption to high-energy side; 737 nm	503.5, 563.3, 596/597, 575, 637, 737, 766.1, 840.7 nm
No defect-related features	No features	503.5, 575, 596/597, 637, 699, 737 nm
No defect-related features	No features	503.5, 540.7, 563.3, 575, 596/597, 637, 737 nm
nd	nd	503.2, 503.5, 575, 596/597, 637, 699, 737 nm
No defect-related features	No features	737 nm
No defect-related features	Broad band at ~261 nm	737, 953 nm

through the entire CVD overgrowth, and was the main cause of the light brown body color. Brown zoning also was observed in the Apollo CVD synthetic diamonds (Wang et al., 2003); it may be caused by concentrated deposition of non-diamond carbon as a result of temperature fluctuations during growth. The presence of non-diamond carbon in the brown sample in this study was revealed by Raman bands at around 1450 cm^{-1}; such bands in CVD-grown diamond are much broader than the Raman peak at 1332 cm^{-1} that is intrinsic to diamond.

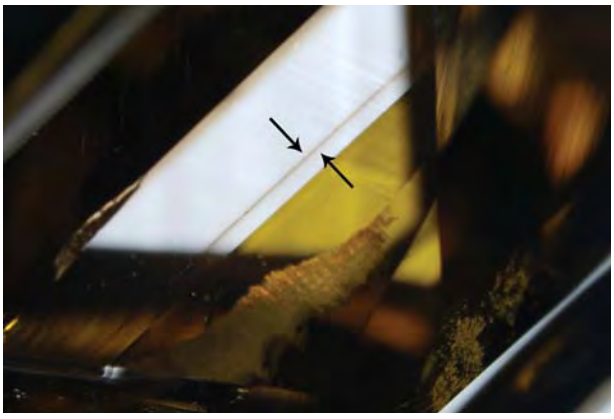
Layers of different colors also have been observed in many CVD products from Element Six. According to Martineau et al. (2004), layers with various brown colors were most common, with blue layers observed in samples doped with boron.

The CVD-grown diamonds were of high clarity. However, a few notable internal features were present. In sample no. 66875, graphite inclusions, identified by Raman spectroscopy, were well developed in the four corners and arranged in the {111} orientation along many small fractures. Although the mechanism responsible for the formation of graphite in these crystals is unclear, it is well known that nitrogen incorporates and degrades the {111} faces preferentially, leading to a higher content of non-diamond carbon. In addition, many pinpoints were present in sample no. 66669.

The main (100) growth surface of the nitrogen-doped samples invariably showed sequences of micro-steps with relatively flat "terrace" regions separated by inclined "risers." This phenomenon is known as step-bunching, and the corresponding features have been referred to as growth steps (de Theije et al., 2000; Martineau et al., 2004). It was observed on all the nitrogen-doped samples (figure 3), and also on portions of high-purity sample 66675 (figure 4). But in the latter case, since no nitrogen was intentionally added, the higher methane concentration present during growth was probably responsible for the surface growth features observed.

Anomalous birefringence, caused by residual internal strain, is a useful feature for the identification of CVD synthetic diamond (see, e.g., Wang et al., 2003; Martineau et al., 2004). Similar to many of the Apollo products examined, the CVD synthetic diamond crystals from LIMHP-CNRS displayed cross-hatched bands of low-order interference colors when viewed through the (100) face (figure 5A). Small areas of localized strain with relatively higher order interference colors surrounding tiny defect centers also were observed. Much higher order interference colors were seen at the four corners in sample no. 66875 (figure 5B), and outside the substrate window in sample 66876 (figure 5C), indicating strong residual internal strain and accumulated dislocations in these regions.

Figure 2. When viewed perpendicular to the growth direction and parallel to the (100) face, CVD synthetic diamond sample no. 67404 displays a dark brown color zone (see arrows) parallel to {100}. The yellow "triangle" to the lower right of the arrows is the substrate of HPHT synthetic diamond. Photomicrograph (taken before substrate was removed) by W. Wang; total thickness of the specimen was 3.36 mm.



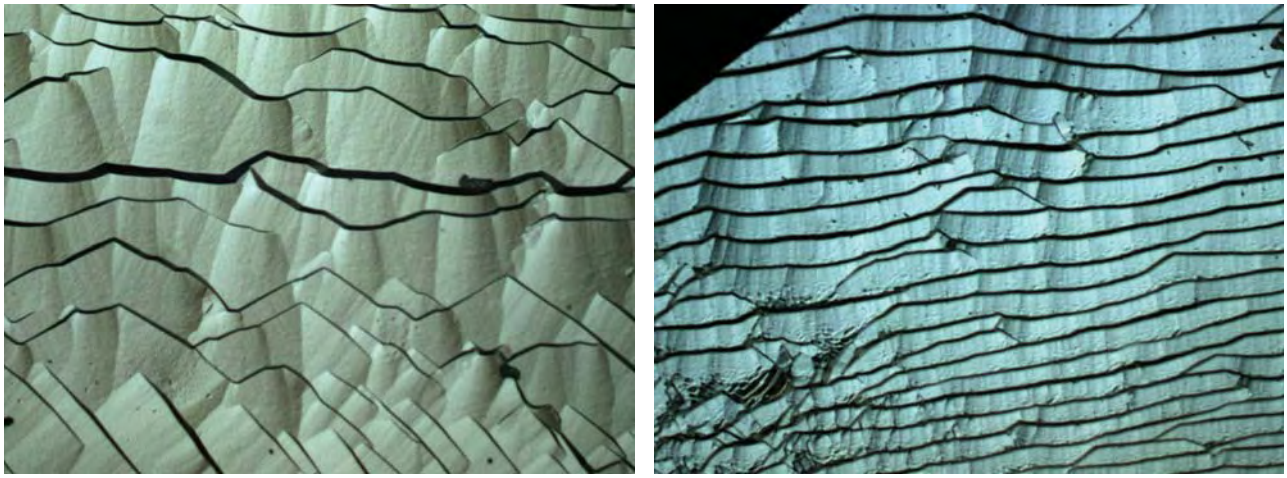


Figure 3. Differential interference contrast microscopy revealed sequences of growth steps with terrace regions separated by inclined risers on the (100) surface of the nitrogen-doped CVD synthetic diamonds (left, no. 67404; right, no. 66875). Photomicrographs by Alexandre Tallaire; magnified 50×.

An outstanding feature evident from the anomalous birefringence is that bundles of dislocations nucleated along the boundary between the substrate and its CVD synthetic diamond overgrowth and are uniformly parallel to the growth direction, as first pointed out by Martineau et al. (2004). As a result, the "shadow" of the substrate can be clearly seen in the birefringence image, even after its removal. This feature was observed in all crystals except for no. 66669.

Figure 4. With a gemological microscope, portions of this high-purity CVD synthetic diamond (no. 66675) display surface growth features similar to those observed on the nitrogen-doped crystals. The apparent color is caused by the yellow substrate of HPHT synthetic diamond, which was not removed. Photomicrograph by W. Wang; image width is approximately 2.9 mm.



In addition, the region outside the substrate "shadow" typically showed higher-order interference colors (figure 5C). Anomalous birefringence caused by residual internal strain is also a common feature of natural type IIa diamond. While large variations in intensity have been observed, natural type IIa diamonds generally show stronger anomalous birefringence than is seen in CVD synthetic diamonds (see, e.g., Moses et al., 1999). Banded and "tatami" patterns are the predominant strain characteristics of natural type IIa diamonds (figure 6, A and B; see, e.g., Smith et al., 2000); as shown in figure 5, the characteristic strain pattern of single-crystal CVD synthetic diamond is distinctly different. HPHT-grown synthetic type IIa diamonds most commonly show no strain (figure 6C).

All five of the samples tested were inert to the UV radiation emitted by a standard gemological UV lamp, and no phosphorescence was observed. In contrast, some of the Apollo nitrogen-doped samples studied by Wang et al. (2003) fluoresced a very weak orange, orange-yellow, or yellow to long-wave UV, and a very weak to moderate orange to orange-yellow to short-wave UV. Orange fluorescence of varying intensity to both long- and short-wave UV radiation was also observed in many of the Element Six nitrogen-doped crystals; in contrast, those of high purity were inert (Martineau et al., 2004). Most natural type IIa diamonds are inert to both long- and short-wave UV. Only a few natural type IIa diamonds are known to fluorescence blue or orange to standard UV radiation. In contrast, most HPHT synthetic type IIa diamonds show weak to moderately strong yellow-green fluorescence and moderate to strong yellow-green phosphorescence to short-wave UV radiation (see, e.g., Shigley et al., 1997).

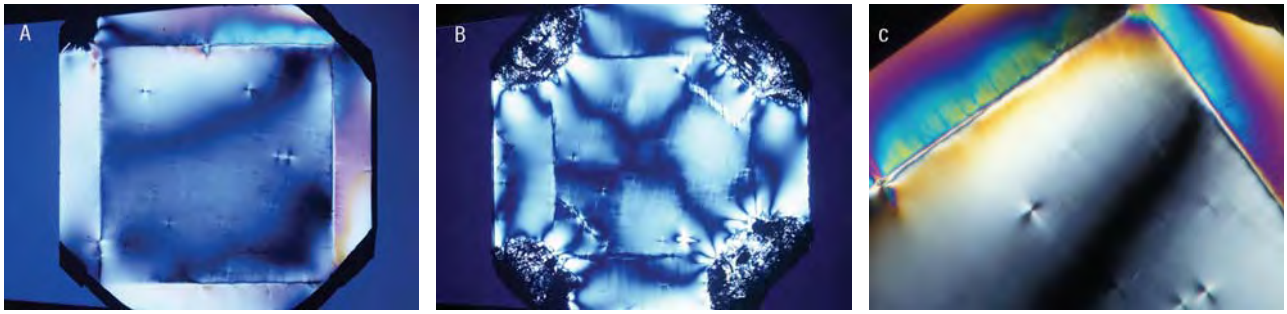


Figure 5. The high-purity crystal in image A (no. 66876), which measures 4.4 mm across, displays the characteristic strain pattern of a CVD-grown diamond when viewed perpendicular to a cubic crystal face (100). The "shadow" of the substrate is clearly visible even after its removal, as the large square with relatively lower order interference colors in the center of the sample. Much higher order interference colors were observed at the four corners of nitrogen-doped sample no. 66875 (B, 6.3 mm across) and in the area outside the substrate "shadow" of sample no. 66876 (C, image width is 2.9 mm), indicating strong residual internal strain and accumulated dislocations in these regions. Photos A and B by W. Wang, and photomicrograph C by Shane McClure; crossed polarizers.

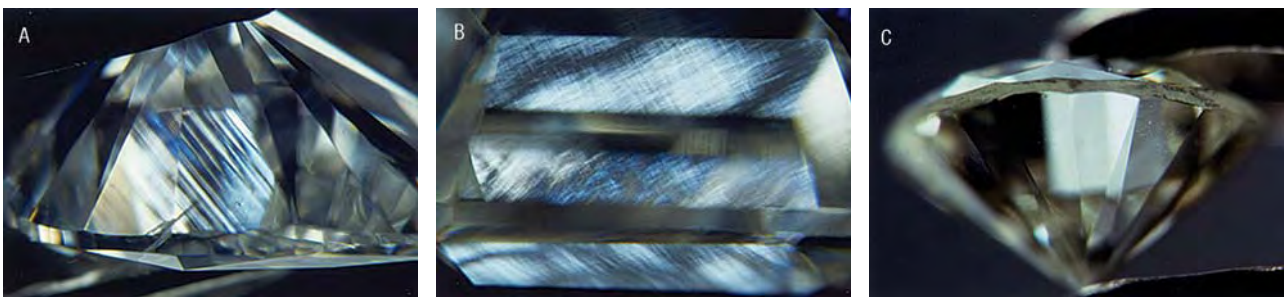
Spectroscopic Features. *Photoluminescence.* PL spectra showed that three of the samples were nitrogen doped and three others were of high purity, as expected from the growth methods employed (see figure 7 and table 1). Several laser excitations were used to obtain maximum sensitivity over various energy regions. Using high-energy 488.0 nm laser excitation allows the detection of trace amounts of 3H, H3, and H4 defects. The 514.5 nm laser system is more sensitive at detecting the 637 nm [$(N\text{-}V)^-$] defect, and 632.8 nm excitation is ideal for detecting traces of Si impurity.

Major PL features in the nitrogen-doped samples include strong emissions of $(N\text{-}V)^0$ with its zero-phonon line (ZPL) at 575 nm and $(N\text{-}V)^-$ with its ZPL at 637 nm, weak emission pairs at 596–597 nm, and Si-related emission at 737 nm (e.g., Bergman et al., 1993).

In two specimens (nos. 66669 and 66875), the intensity of the 637 nm emission was stronger than or close to that of the 575 nm. However, the other nitrogen-doped sample (no. 67404) showed the opposite trend. During crystal growth, samples 66669 and 66875 were doped with moderate and low nitrogen contents, respectively. In contrast, sample 67404 was doped with only a very small amount of nitrogen. It seems that the higher the nitrogen content is, the higher the intensity of the 637 nm emission compared to that of the 575 nm will be. When 488 nm laser excitation was employed, the integrated intensity ratio (i.e., the area of a peak, rather than its height) of 637/575 was 1.31 for sample 66669, 0.96 for sample 66875, and only 0.07 for sample 67404. These observations indicate a possible correlation between the content of doped nitrogen and the concentrations of $(N\text{-}V)^0$ and $(N\text{-}V)^-$ centers generated. They are consistent with the suggestion that $(N\text{-}V)^0$ is initially incorporated during CVD growth, and $(N\text{-}V)^-$ appears and intensifies as the nitrogen content further increases (M. Newton, pers comm., 2005).

In contrast to the nitrogen-doped CVD synthetic diamonds, the two high-purity samples (nos. 66876 and 67405) displayed virtually no PL features. Only

Figure 6. In contrast to CVD synthetic diamonds, natural type IIa diamonds typically show banded and "tatami" patterns with low first-order interference colors (A, B). HPHT-grown synthetic type IIa diamonds most commonly show no strain (C). Photomicrographs by Christopher Smith; crossed polarizers.



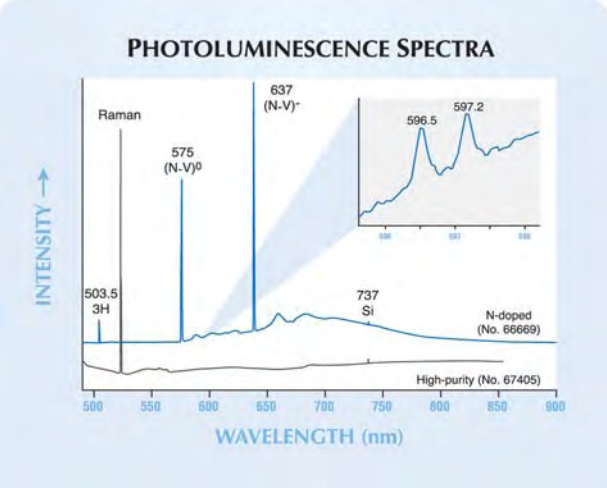


Figure 7. Low-temperature photoluminescence spectra collected using an Ar-ion laser (488 nm excitation) revealed clear differences between the nitrogen-doped and high-purity CVD synthetic diamonds. Strong emissions at 575 and 637 nm—and weak emissions at 503.5, 596, 597, and 737 nm—were detected in the three nitrogen-doped samples. Three high-purity CVD synthetic diamonds displayed only a very weak emission at 737 nm caused by trace Si impurity, although this emission was extremely strong in one N-doped sample (no. 67404).

a very weak 737 nm emission was detected. Nevertheless, it appears that the high-purity crystals from LIMHP-CNRS are slightly less pure than those from Element Six examined by Martineau et al. (2004), in which no Si-related emission was detected. Sample no. 67405 also showed a very weak emission line at 953 nm when 780 nm laser excitation was employed. High-purity crystal no. 66675 displayed very weak emissions at 575 nm and 637 nm, which are very likely from its type Ib HPHT synthetic diamond substrate. This explanation is supported by the occurrence of a very weak H3 emission (zero phonon line at 503.2 nm), which certainly is from the substrate.

In addition, very weak emissions at 563, 699, 766, and 841 nm were occasionally observed in the LIMHP-CNRS samples (again, see table 1). The 3H defect, with a zero-phonon-line position at 503.5 nm (slightly higher than that of H3 at 503.2 nm), is typically radiation related (Collins et al., 1989). The 3H defect is relatively unstable, and should be annealed out at typical CVD growth temperatures (Zaitsev, 2001); nevertheless, the 3H defect was detected in all three nitrogen-doped crystals and in one high-purity crystal (no. 66675). In contrast, the 3H defect was not detected in any of the Apollo

Figure 8. Except for brown sample no. 67404, the CVD synthetic diamonds from LIMHP-CNRS did not show any defect-related absorption in the mid-infrared range. Sharp, very weak absorptions at 3323 and 3124 cm^{-1}, and two relatively broad absorptions at 2924 and 2807 cm^{-1}, were detected in sample no. 67404. In contrast, these H-related absorptions were observed in many of the Apollo CVD synthetic diamonds examined by Wang et al. (2003). The spectra are shifted vertically for clarity.

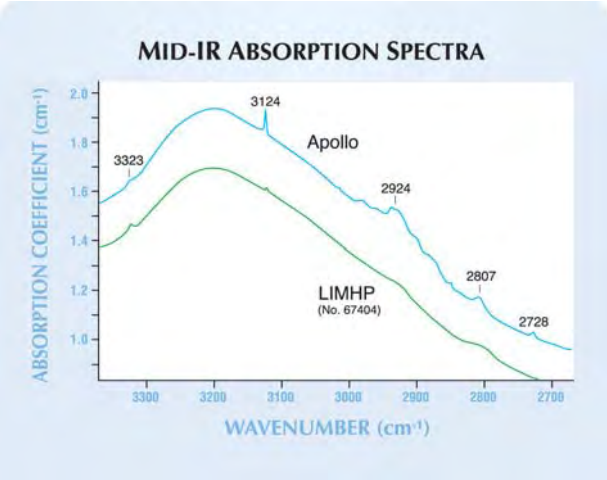
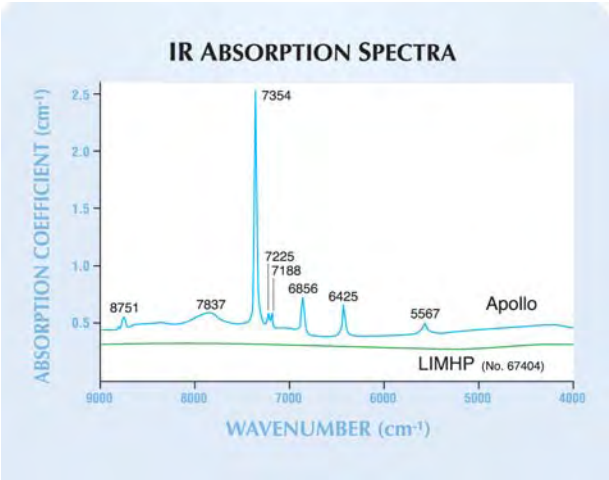


Figure 9. The CVD synthetic diamonds from LIMHP-CNRS did not show any defect-related absorption in the near-infrared range. In contrast, most Apollo CVD synthetic diamonds examined by Wang et al. (2003) displayed relatively strong absorptions in this range. Of the five specimens examined, only the light brown crystal (no. 67404) exhibited a very weak absorption at 6856 cm^{-1} (not visible below). The spectra are shifted vertically for clarity.



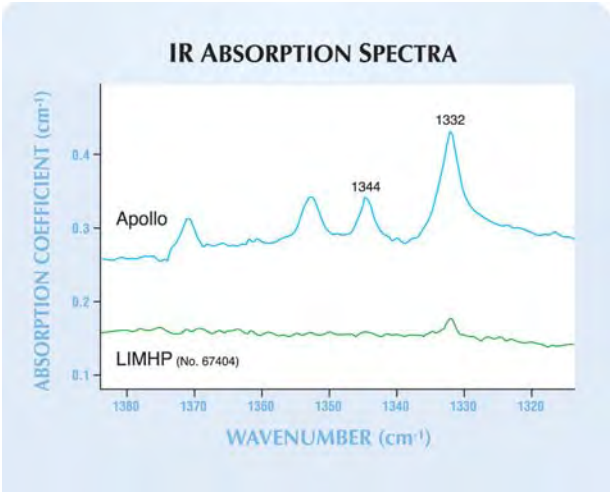


Figure 10. None of the CVD synthetic diamonds from LIMHP-CNRS examined showed the absorption at 1344 cm^{-1} associated with trace amounts of isolated nitrogen, which was present in several of the Apollo CVD synthetic diamonds studied by Wang et al. (2003). The spectra are shifted vertically for clarity.

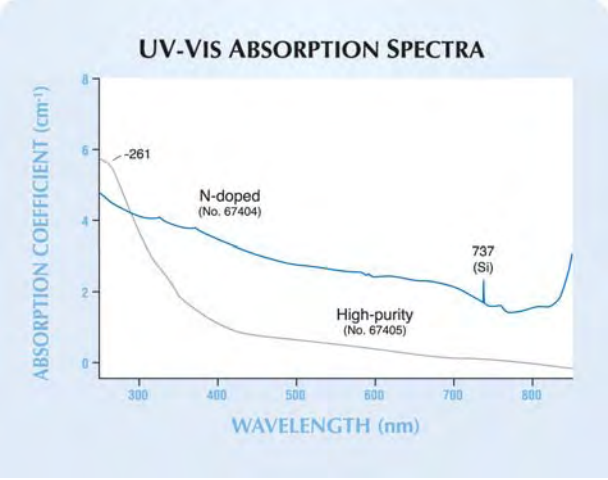
products (Wang et al., 2003) or reported by Martineau et al. (2004) for CVD synthetic diamond samples produced by Element Six.

This apparent discrepancy might be explained by the fact that two of the nitrogen-doped crystals (nos. 66875 and 66669) and one high-purity crystal (no. 66876) had previously been analyzed by cathodoluminescence, which can introduce weak radiation damage (Steed et al., 1999). However, no 3H features were detected in high-purity crystal no. 66876, while nitrogen-doped crystal no. 67404 was not analyzed with any method involving cathodoluminescence or X-radiation but also showed a weak 3H. Still, the presence of the 3H defect in four crystals examined in this study is not likely to be an as-grown feature but rather may have been introduced accidentally afterwards, perhaps by exposure to X-rays in an airport security checkpoint.

IR Spectroscopy. Infrared absorption spectroscopy revealed that all samples were type IIa. Except for the light brown crystal (no. 67404), no defect-related absorptions were detected in the infrared region (figures 8 and 9). In contrast, the Apollo products examined by Wang et al. (2003) and the nitrogen-doped Element Six CVD synthetic diamond samples studied by Martineau et al. (2004) usually showed strong hydrogen-related absorptions in both the mid- and near-infrared regions. In the LIMHP-CNRS samples, weak, sharp absorptions at 3323 and 3124 cm^{-1}, and two broad absorptions at 2924 and 2807 cm^{-1}, were observed only in the light brown crystal. In addition, none of the crystals examined showed any absorption due to trace amounts of isolated nitrogen at 1344 cm^{-1} (figure 10), which was present in many of the Apollo CVD synthetic diamonds examined by Wang et al. (2003). Hydrogen-related absorptions in the infrared region were important identification features for the Apollo CVD synthetic diamonds, since many of these features are specific to CVD synthesis (Martineau et al., 2004). However, they were not diagnostic for the CVD synthetic diamonds in this study.

UV-Vis-NIR Spectroscopy. Low-temperature absorption spectra collected in the UV-Vis-NIR range revealed few notable features (figure 11). Spectra from the high-purity and the near-colorless nitrogen-doped samples were very flat in the visible range, and increased gradually into the UV region. A weak and broad band at ~261 nm was detected in sample no. 67405; its assignment is not certain, but

Figure 11. The low-temperature absorption spectrum of this high-purity CVD synthetic diamond (no. 67405) is rather flat in the visible-light range, and increases gradually in the UV region. The assignment of a weak and broad band at ~261 nm is not clear, but this absorption is likely not due to isolated nitrogen. In the brown nitrogen-doped CVD-grown diamond (no. 67404), the absorption increases gradually toward lower wavelengths. A distinct absorption at 737 nm due to a Si impurity also was observed. The spectra are shifted vertically for clarity.



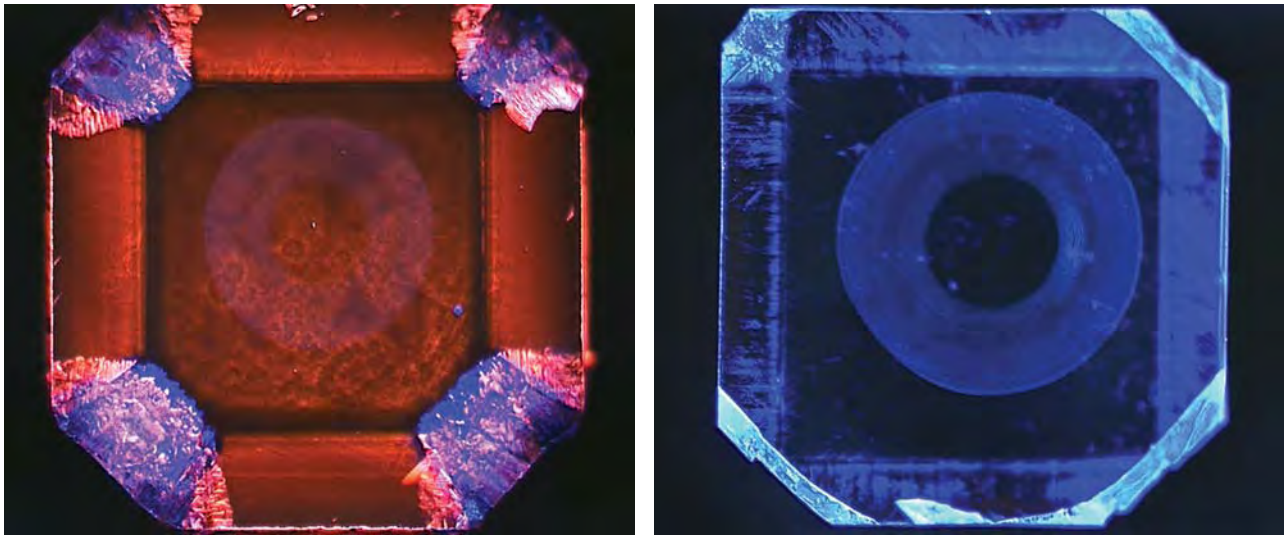


Figure 12. In the DTC DiamondView, the nitrogen-doped CVD-grown crystals showed a strong and characteristic orange to orangy red luminescence (sample no. 66875, left). In contrast, the high-purity crystals showed only a very weak blue fluorescence (sample no. 66876, right). The original positions of the substrates are visible as the darker square-shaped patterns in the center of the images. The circular areas within the squares are from the sample holder. Photos by W. Wang.

the band is most likely not due to isolated nitrogen (Zaitsev, 2001). In the light brown nitrogen-doped CVD-grown diamond (no. 67404), the absorption increased gradually toward lower wavelengths. A distinct absorption at 737 nm (0.64 cm^{-1} absorption coefficient) was also observed in this sample. The intensity of this peak was stronger than that of all the Apollo products we have examined so far. Early products from Element Six showed an emission line at 737 nm in the photoluminescence spectrum, but its absorption intensity was not reported. In addition, this feature was not detected in samples grown more recently by Element Six (Martineau et al., 2004).

DiamondView Imaging. When examined with the DiamondView, the nitrogen-doped samples exhibited strong orange to orangy red luminescence due to both $(N\text{-}V)^0$ and $(N\text{-}V)^-$ centers (figure 12, left). In contrast, the high-purity synthetic crystals luminesced very weak blue (figure 12, right). The blue luminescence is believed to emanate from bundles of dislocations in arrangements not seen in natural diamond (Martineau et al., 2004). In figure 12 (left), blue luminescence also can be seen at the four corners of nitrogen-doped crystal no. 66875, where extensive dislocations appeared in the anomalous birefringence image (figure 5B).

Two crystals showed blue phosphorescence in the DiamondView. One (no. 67404) was nitrogen doped (figure 13, left), and the other (no. 67405) was of high purity (figure 13, right). Blue phosphorescence is common in many natural type IIb diamonds and may also occur in some HPHT-grown synthetic type IIa diamonds (Shigley et al., 1997; King et al., 1998), but it is rarely seen in

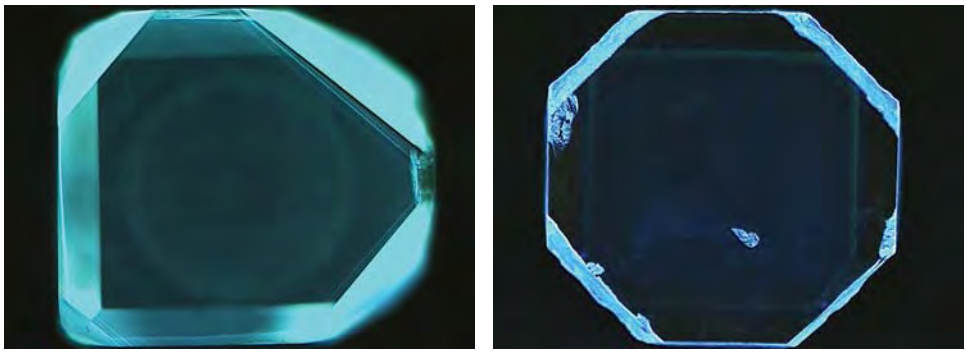


Figure 13. In the DiamondView, two of the studied CVD samples (left, no. 67404; right, no. 67405) showed moderately strong blue phosphorescence, which is rarely observed in natural type IIa diamonds. Photos by W. Wang.

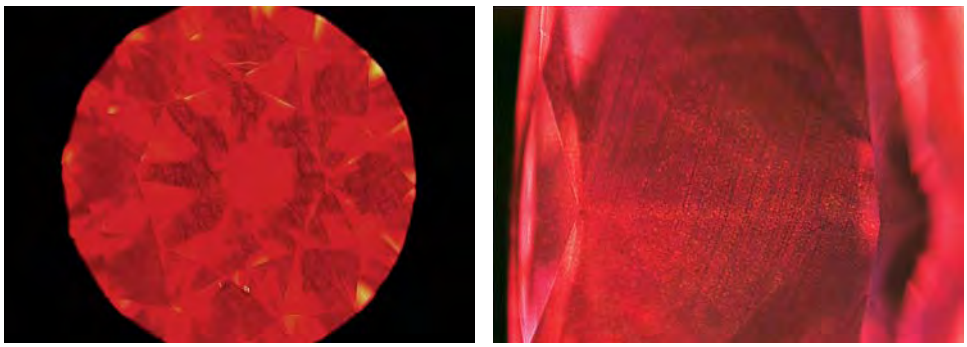


Figure 14. Characteristic "mosaic" networks of polygonized dislocations (left, 6.44 mm in diameter) and dislocations lying in slip bands (right, 3.9 mm depth) are the major features of natural type IIa diamonds with orange fluorescence seen in the DiamondView. Photos by W. Wang (left) and Paul Johnson (right).

natural type IIa diamonds. As in the aforementioned birefringence images, the original position of the HPHT-grown synthetic substrate also was observable in most DiamondView fluorescence and phosphorescence images.

Natural type IIa diamonds usually show blue fluorescence in the DiamondView, and they typically display characteristic "mosaic" networks of polygonized dislocations or dislocations lying in slip bands (Martineau et al., 2004). A few natural type IIa diamonds exhibit orange luminescence, similar to that of nitrogen-doped CVD synthetic diamonds. Our extensive examinations have revealed that "mosaic" networks and slip bands are also the predominant features of natural type IIa diamonds that show this orange fluorescence (figure 14).

IDENTIFICATION FEATURES

The CVD synthetic diamonds from LIMHP-CNRS were produced solely for research purposes, but in the event a similar product ultimately reaches the gem market it is important to understand the differences between these samples and natural diamonds, as well as other gem-quality CVD synthetics currently being produced. Although the products examined in this study showed considerable variation in color and purity, it is clear that deposition of non-diamond carbon during crystal growth at relatively high growth rates can be minimized, leading to the formation of near-colorless gem-quality crystals. The relatively narrow thickness of CVD overgrowth (no more than 1.64 mm in the crystals examined) would limit their potential jewelry application to very small gems. However, other manufacturers (Apollo Diamond, Element Six, and the Carnegie Institute) have demonstrated their ability to grow high-quality CVD crystals thick enough to be faceted as gems. It is feasible that LIMHP-CNRS has a similar capability.

The new LIMHP-CNRS synthetic diamonds showed distinct differences in optical and spectroscopic properties from the suite of Apollo products examined by Wang et al. (2003), as well as from the Element Six CVD samples examined by Martineau et al. (2004). Fortunately, the LIMHP-CNRS samples we examined could be identified on the basis of their characteristic birefringence images, orange or blue luminescence features in the DiamondView, and/or PL spectroscopic features (i.e., emission at 737 nm and a 596/597 nm pair). Very few natural type IIa diamonds fluoresce orange or orangy red in the DiamondView, so this reaction is a good indication that further testing is necessary. One CVD-specific PL spectroscopic feature is the weak doublet at 596 and 597 nm, which was detected in all three nitrogen-doped samples and in one high-purity CVD crystal in this study. More importantly, the Si-related defect at 737 nm, which has never been reported in natural diamonds, occurred at varying intensity in all the samples (both nitrogen doped and high purity) examined in this study, making it a very useful identification feature.

CONCLUDING REMARKS

CVD synthetic diamonds from LIMHP-CNRS have been created solely for research purposes, as both nitrogen-doped and high-purity samples. These type IIa products showed considerable variation in color and impurity concentration. This study revealed some subtle but clear differences between the LIMHP-CNRS products and the suite of Apollo products examined by Wang et al. (2003) and the Element Six products examined by Martineau et al. (2004). While the LIMHP-CNRS synthetics show almost no absorption features in the infrared

region, they can be reliably identified based on their characteristic birefringence images, luminescence features in the DiamondView, and/or PL spectroscopic features.

With the rapid progress in CVD growth techniques, larger and better-quality synthetic diamonds are likely to be produced. Identification features will probably change to some extent with the continued development of CVD synthesis techniques.

ABOUT THE AUTHORS

Dr. Wang (wuyi.wang@gia.edu) is research scientist, Mr. Hall is manager of analytical research services, and Mr. Moses is vice president of Identification and Research at the GIA Laboratory in New York. Mr. Tallaire is a PhD student, Dr. Achard is associate professor, and Dr. Gicquel is professor and leader of the diamond group at the LIMHP-CNRS, Université Paris 13, France. Dr. Sussmann is senior research fellow at King's College London, United Kingdom.

ACKNOWLEDGMENTS: The authors are grateful to Dr. James Butler of the Naval Research Laboratory, Washington, DC, and Dr. Mark Newton of the University of Warwick, Coventry, U.K., for many helpful discussions. Christopher Smith, Shane McClure, Thomas Gelb, Dr. James Shigley, Dr. Mary Johnson, Dr. Christopher Breeding, and Dr. Andy Hsi-Tien Shen of the GIA Laboratory are thanked for their observations and comments.

REFERENCES

Bates R. (2005) University claims "better, faster" synthetic diamonds. *JCK*, Vol. 176, No. 6, p. 51

Bergman L., Stoner B.R., Turner K.F., Glass J.T., Nemanich R.J. (1993) Microphotoluminescence and Raman scattering study of defect formation in diamond films. *Journal of Applied Physics*, Vol. 73, No. 8, pp. 3951–3957.

Collins A.T., Kamo M., Sato Y. (1989) Optical centers related to nitrogen, vacancies and interstitials in polycrystalline diamond films grown by plasma-assisted chemical vapour deposition. *Journal of Physics D: Applied Physics*, Vol. 22, No. 9, pp. 1402–1405.

de Theije F.K., Schermer J.J., van Enckevort W.J.P. (2000) Effects of nitrogen impurities on the CVD growth of diamond: Step bunching in theory and experiment. *Diamond and Related Materials*, Vol. 9, No. 8, pp. 1439–1449.

King J.M., Moses T.M., Shigley J.E., Liu Y. (1994) Color grading of colored diamonds at the GIA Gem Trade Laboratory. *Gems & Gemology*, Vol. 30, No. 4, pp. 220–242.

King J.M., Moses T.M., Shigley J.E., Welbourn C.M., Lawson S.C., Cooper M. (1998) Characterizing natural-color type IIb blue diamonds. *Gems & Gemology*, Vol. 34, No. 4, pp. 246–268.

Martineau P.M., Lawson S.C., Taylor A.J., Quinn S.J., Evans D.J.F., Crowder M.J. (2004) Identification of synthetic diamond grown using chemical vapor deposition (CVD). *Gems & Gemology*, Vol. 40, No. 1, pp. 2–25.

Moses T.M., Shigley J.E., McClure S.F., Koivula J.I., Van Daele M. (1999) Observations on GE-Processed Diamonds: A photographic record. *Gems & Gemology*, Vol. 35, No. 3, pp. 14–22.

Shigley J.E., Fritsch E., Stockton C.M., Koivula J.I., Fryer C.W., Kane R.E. (1986) The gemological properties of the Sumitomo gem-quality synthetic yellow diamonds. *Gems & Gemology*, Vol. 22, No. 4, pp. 192–208.

Shigley J.E., Fritsch E., Stockton C.M., Koivula J.I., Fryer C.W., Kane R.E., Hargett D.R., Welch C.W. (1987) The gemological properties of the De Beers gem-quality synthetic diamonds. *Gems & Gemology*, Vol. 23, No. 4, pp. 187–206.

Shigley J.E., Moses T.M., Reinitz I., Elen S., McClure S.F., Fritsch E. (1997) Gemological properties of near-colorless synthetic diamonds. *Gems & Gemology*, Vol. 33, No. 1, pp. 42–53.

Shigley J.E., Abbaschian R., Clarke C. (2003) Gemesis laboratory-created diamonds. *Gems & Gemology*, Vol. 38, No. 4, pp. 301–309.

Shigley J.E., McClure S.F., Breeding C.M., Shen A., Muhlmeister S.M. (2004) Lab-grown colored diamonds from Chatham Created Gems. *Gems & Gemology*, Vol. 40, No. 2, pp. 128–145.

Smith C.P., Bosshart G., Ponahlo J., Hammer V.M.F., Klapper H., Schmetzer K. (2000) GE POL diamonds: Before and after. *Gems & Gemology*, Vol. 36, No. 3, pp. 192–215.

Steed J.W., Davis T.J., Charles S.J., Hayes J.M., Butler J.E. (1999) 3H luminescence in electron-irradiated diamond samples and its relationship to self-interstitials. *Diamond and Related Materials*, Vol. 8, No. 10, pp. 1847–1852.

Tallaire A., Achard J., Sussmann R.S., Silva F., Gicquel A. (2005) Homoepitaxial deposition of high-quality thick diamond films: Effect of growth parameters. *Diamond and Related Materials*, Vol. 14, No. 3–7, pp. 249–254.

Wang W., Moses T., Linares R., Shigley J.E., Hall M., Butler J.E. (2003) Gem-quality synthetic diamonds grown by the chemical vapor deposition method. *Gems & Gemology*, Vol. 39, No. 4, pp. 268–283.

Welbourn C.M., Cooper M., Spear P.M. (1996) De Beers natural versus synthetic diamond verification instruments. *Gems & Gemology*, Vol. 32, No. 3, pp. 156–169.

Yan C.-S., Vohra Y.K., Mao H.-K., Hemley R.J. (2002) Very high growth rate chemical vapor deposition of single-crystal diamond. *Proceedings of the National Academy of Sciences of the United States of America*, Vol. 99, No. 20, pp. 12523–12525.

Yan C.-S., Chen Y.-C., Ho S.-S., Mao H.-K., Hemley R.J. (2005) Large single crystal CVD diamonds at rapid growth rates. *Abstracts of the 8th Applied Diamond Conference/NanoCarbon 2005*, May 15–19, Argonne National Laboratory, Argonne, Illinois.

Zaitsev A.M. (2001) *Optical Properties of Diamond*. Springer-Verlag, Berlin, 502 pp.